

Identifying the Group to Intervene on to Maximise Effect Under Cross-Group Interference

Xiaojing Du, Jiuyong Li, Lin Liu, Debo Cheng, Jixue Liu, Thuc Duy Le
Adelaide University
Adelaide, SA, Australia

Abstract

In many networked systems, interventions applied to one group of units can induce substantial causal effects on another group through cross-group interference pathways. Despite its practical importance in domains such as public health, digital marketing, and social policy, the problem of identifying which intervention subset in a source group maximizes the benefit on a target group remains largely unaddressed. We formalize this problem as *cross-group causal influence estimation* and introduce the *core-to-group causal effect* (Co2G), a formally defined causal estimand that quantifies the contrast in target-group outcomes under intervention versus non-intervention on a candidate source subset. We establish the nonparametric identifiability of Co2G from observational network data using do-calculus under standard causal assumptions, and develop a graph neural network-based estimator that captures cross-group interference patterns. To navigate the combinatorial search space of candidate subsets, we propose *CauMax*, an uncertainty-aware causal effect maximization framework with two scalable selection algorithms: (i) *CauMax-G*, an iterative greedy search with Monte Carlo dropout-based lower confidence bounds, and (ii) *CauMax-D*, a differentiable gradient-based optimization via Gumbel–Softmax relaxation. Extensive experiments on two real-world social networks demonstrate that *CauMax* achieves an order-of-magnitude reduction in regret compared with structural heuristics and diffusion-based baselines, and that moderate uncertainty penalization consistently improves subset selection quality.

CCS Concepts

• **Computing methodologies** → **Learning in probabilistic graphical models.**

Keywords

Causal Inference, Network Interference, Cross-Group Spillover Effects, Causal Effect Maximization, Subset Intervention

1 Introduction

In many real-world systems, interventions applied to one group of entities can induce substantial causal effects on other distinct groups through complex interaction structures. Such phenomena arise broadly in social [32], economic [9], biological [21], and online systems [33], where individuals or units are embedded in networks that mediate indirect effects across group boundaries. In these settings, an intervention targeting a subset of units may influence outcomes of other units that are not directly treated, giving rise to interference and violating the standard assumption that each unit’s outcome depends only on its own treatment assignment. Understanding and quantifying causal effects under interference has

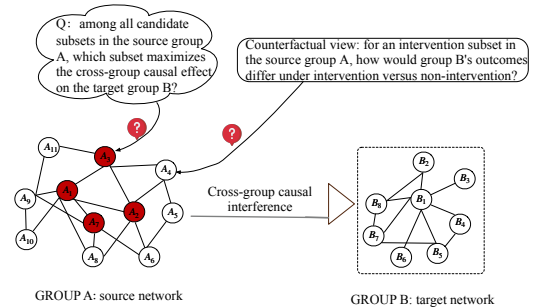


Figure 1: Illustration of the cross-group causal interference problem. The source group A forms a complex interaction structure, and an intervention can be applied to any candidate subset. The goal is to identify the subset that creates the maximal effect on target group B . The causal mechanism operates through cross-group interference pathways from A to B . For a subset, the counterfactual perspective compares the target group-level outcomes under intervention and non-intervention on a subset. Red nodes denote a candidate intervention subset.

therefore become a central challenge in modern causal inference on networked data [12, 13, 23].

One prominent motivating domain where cross-group causal interference plays a crucial role is epidemiology. Epidemiological studies have long shown that the role of *core transmitters* in the spread of infectious diseases far exceeds their proportion in the population [1, 3]. Although core groups, such as highly connected individuals or central clusters in epidemiological networks, represent only a small fraction of the population, their high contact rates and concentrated interactions make them the dominant sources of transmission. Consequently, disease spread is highly heterogeneous rather than uniform across populations, and interventions targeting highly connected regions can induce spillover effects that propagate widely through social contact networks [6, 27]. These findings highlight a fundamental methodological challenge: under network interference, how can we formally identify which core groups generate the largest causal influence, particularly when their own group produces cross-group spillovers? Understanding such cross-group causal influence is crucial for designing targeted interventions in real-world systems where social, behavioral, or biological interactions routinely span community boundaries.

Motivating Example 1. Public vaccination programs offer a compelling illustration of how interventions targeted at one population segment can generate substantial causal effects on another. In many regions, elderly individuals or patients with severe chronic

Table 1: Representative works related to network interference and influence.

Representative Works	Cross-Group	Causal Effect Max.
Jiang and Sun [16]	✗	✗
Cai et al. [4]	✗	✗
Aronow and Samii [2]	✗	✗
Ogburn et al. [23]	✗	✗
Miguel and Kremer [22]	✓	✗
Heitzig and O’Keeffe-O’Donovan [10]	✓	✗
Ji et al. [15]	✓	✗
Possnig et al. [25]	✗	✗
Lee et al. [19]	✗	✗
Su et al. [30]	✗	✓
Ours	✓	✓

conditions cannot be directly vaccinated, making their protection dependent on interventions targeting other core sources of transmission, such as highly connected working-age adults or densely interacting social groups. Vaccinating a particular core subgroup reduces its members’ infection risk and, crucially, lowers disease transmission to elderly communities that remain unvaccinated. Different choices of core groups lead to markedly different target benefits, as each subgroup interacts with the elderly through distinct contact patterns and transmission pathways. These indirect protective effects constitute a form of cross-group causal influence, as illustrated in Figure 1. The key challenge is that observed infection outcomes among the elderly reflect only the intervention actually implemented, whereas policy decisions require understanding how these outcomes would have differed under alternative intervention choices and identifying the one that maximizes the causal benefit on the target.

Motivating Example 2. Digital product ecosystems often exhibit cross-group influence, where interventions applied to one community reshape the behavior of another. Consider a company launching a new AI-powered note-taking application and seeking to increase adoption among students. Because direct intervention on students is limited, the company instead provides a free premium version to selected online content creators. Treating these creators increases their own usage and encourages them to feature the product in their content, indirectly exposing the target student community and raising adoption without direct intervention. Importantly, creators differ substantially in their target impact: only a small subset may strongly influence students’ adoption decisions. However, the company observes outcomes only under the intervention applied to a given set of creators. Effective decision making therefore requires understanding how student adoption would have differed had the intervention targeted alternative creator subsets, a fundamentally counterfactual question involving cross-group causal influence.

These intertwined diffusion mechanisms highlight the limitations of existing causal inference frameworks under network interference. As summarized in Table 1, most previous studies either confine spillovers within a single community [2, 4, 16, 23] or fail to capture the asymmetric influence exerted by highly active core groups [10, 15, 22, 25]. While recent work has begun to formalize influential individuals’ causal influence, such as Lee et al. [19] who propose a causal framework to identify influential subjects within

a single network, their formulation restricts interference to occur within rather than across groups and does not characterize how interventions propagate between communities. In parallel, Su et al. [30] investigate the environmental sensitivity of influence maximization gains, but their analysis is grounded in algorithmic diffusion models rather than causal estimates, and thus cannot distinguish marginal structural influence from genuine causal spillovers or capture how activation effects transmit across heterogeneous groups. Consequently, existing approaches cannot identify which core sources generate the largest cross-group causal influence, a capability essential for targeting interventions in realistic settings where communities interact, overlap, and exert asymmetric effects on one another.

While classical greedy influence-maximization (IM) methods aim to select seeds that maximize the expected cascade size under a pre-specified diffusion model [5, 17], this perspective fundamentally differs from our objective. Greedy IM algorithms simulate how activation spreads under assumed diffusion dynamics, whereas we seek to determine how outcomes in group B would change under different choices of core sources to target in group A. This distinction is crucial: even perfectly predicting the observed diffusion cannot reveal how group B would have responded had an alternative subset in group A been selected, because such responses correspond to potential outcomes that are never observed in real data [13, 26]. Therefore, identifying the core source that maximizes cross-group improvements requires a causal formulation rather than a purely diffusion-based or algorithmic one. A causal perspective explicitly defines the estimand of interest, clarifies what is identifiable from observational data, and enables principled comparison across intervention choices that were not carried out.

However, identifying which source subset yields the greatest target improvement poses two fundamental challenges. **(a) Unbiased estimation under cross-group interference.** Because treatments assigned to units in a subset in the source network A spill over to units in B through complex network pathways, the potential outcomes corresponding to alternative subsets cannot be observed simultaneously. Standard estimators conflate causal spillovers with correlations induced by network structure or confounding, making the underlying causal contrast difficult to identify from observational data. **(b) The combinatorial search space of intervention choices.** The number of possible subsets grows exponentially with $|A|$, rendering exhaustive evaluation of all counterfactual outcomes infeasible. Classical influence-maximization heuristics are not directly applicable, as they optimize expected cascade sizes under assumed diffusion models rather than causal estimands defined over unobserved potential outcomes. Together, these challenges motivate the need for a framework that (i) identifies unbiased cross-group causal effects from observational network data and (ii) efficiently discovers the subset that maximizes target improvement.

Motivated by these observations, we formulate the problem of cross-group causal influence maximization, which seeks to identify the core sources whose selection for intervention yields the greatest causal improvements in the outcomes of other groups. Our main contributions are summarized as follows:

- **Problem formulation.** We formalize the problem of cross-group causal influence maximization and define the core-to-group causal effect (Co2G), a causal estimand that quantifies the target-group outcome improvement attributable to intervening on a source subset under network interference.
- **Nonparametric identifiability.** We establish the identifiability of Co2G from observational network data using do-calculus under standard graphical causal assumptions, without imposing parametric restrictions on the outcome model.
- **Estimation and optimization framework.** We propose *CauMax*, a causal effect maximization framework that integrates a graph neural network-based estimator for cross-group interference with an uncertainty-aware optimization objective based on Monte Carlo dropout. We instantiate two scalable subset selection algorithms: *CauMax-G*, an iterative greedy search, and *CauMax-D*, a differentiable gradient-based method via Gumbel–Softmax relaxation.
- **Empirical evaluation.** Extensive experiments on BlogCatalog and Flickr demonstrate that the proposed framework achieves an order-of-magnitude reduction in regret over structural and diffusion-based baselines, and that moderate uncertainty penalization consistently improves selection quality.

2 Related Work

Our work lies at the intersection of causal inference under network interference and influence maximization on social networks. We review each line of work below.

2.1 Cross-Group Spillovers in Networked Systems

Classical causal inference under interference has primarily operated under the *partial interference* assumption [11, 28], where spillovers occur only within pre-defined clusters. Extensions to networked observational data [2, 7, 23] allow more flexible interference structures but remain confined to within-group or neighborhood-level effects.

More recent work has examined spillovers that propagate *across* distinct communities. Miguel and Kremer [22] provided early empirical evidence of cross-school treatment externalities in deworming programs. Heitzig and O’Keeffe-O’Donovan [10] documented cross-village diffusion of savings groups, and Ji et al. [15] revealed heterogeneous within- and cross-group spillover effects in influencer marketing. On the estimation side, Jiang and Sun [16] and Cai et al. [4] developed representation learning-based estimators and generalization bounds for causal effects on networked data, though their formulations do not explicitly distinguish source and target groups or model asymmetric cross-group interference. In contrast, our framework formalizes a directional cross-group causal structure where interventions on a source group propagate to a target group through inter-group network connections, and introduces a combinatorial optimization objective over causal estimands.

2.2 Influence Maximization

Influence maximization (IM) selects seed nodes to maximize expected cascade spread under diffusion models such as IC and LT [5, 17, 20]. Recent work has begun to connect IM with causal reasoning: Lee et al. [19] proposed a causal framework for identifying influential subjects within a single network, while Su et al. [30] incorporated individual treatment effects into IM to capture environmental sensitivity of node-level gains.

However, IM fundamentally differs from our objective. IM algorithms optimize expected activation counts under assumed diffusion dynamics, whereas we optimize a formally defined causal estimand the core-to-group causal effect (Co2G) over unobserved potential outcomes. Even perfect diffusion prediction cannot reveal how the target group would have responded under alternative intervention subsets, as these correspond to counterfactual outcomes never observed in data [13, 26]. Our framework bridges this gap by combining causal identification with subset optimization over estimated causal effects.

3 Problem Setup and Cross-Group Interference

Notation. Let V_A denote the set of source-group nodes and V_B denote the set of target-group nodes. A (candidate) intervention subset is denoted by $S \subseteq V_A$ with a budget constraint $|S| \leq K$. We use \mathcal{S} to denote a collection of evaluated subsets (e.g., randomly sampled subsets of varying sizes) in empirical evaluation. For a fixed size k , let S_k denote the subset returned by an algorithm, and let S_k^* denote the oracle optimal subset under the ground-truth causal effect.

Networked Groups and Interference Structure. We consider two disjoint groups of units: a *source group* and a *target group*, corresponding to node sets V_A and V_B , respectively. Edges may exist both within groups and across groups, forming an interaction graph through which influences originating in the source group may propagate to the target group via direct or indirect pathways. The interference pattern is asymmetric: interventions applied to units in group A may affect outcomes in group B , but not vice versa. Such directional cross-group influence patterns arise naturally in many real-world settings, including vaccination and infectious disease control [16, 22], influencer marketing and information diffusion [15, 19], and core–periphery or hierarchical social systems [17, 27].

Subset-Level Intervention. We focus on deterministic joint interventions applied to a subset $S \subseteq V_A$. All units in S are simultaneously assigned to the same treatment level, while units in $V_A \setminus S$ are fixed at a baseline (control) level. Throughout the paper, we assume a binary treatment with levels $t \in \{0, 1\}$ and fix the baseline level as $t_0 = 0$. Our objective is to identify, among a combinatorial space of candidate subsets $S \subseteq V_A$, the subset-level intervention that maximizes the causal effect on the target group B .

Interventional Target-Group Mean. Let Y_j denote the outcome of target node $j \in V_B$, and define the average target-group outcome as $Y_B = \frac{1}{|V_B|} \sum_{j \in V_B} Y_j$. For any subset $S \subseteq V_A$ and treatment level $t \in \{0, 1\}$, we define the *interventional target-group mean* as

$$\mu_B(t; S) := \mathbb{E}[Y_B \mid \text{do}(T_S = t), \text{do}(T_{V_A \setminus S} = t_0)], \quad (1)$$

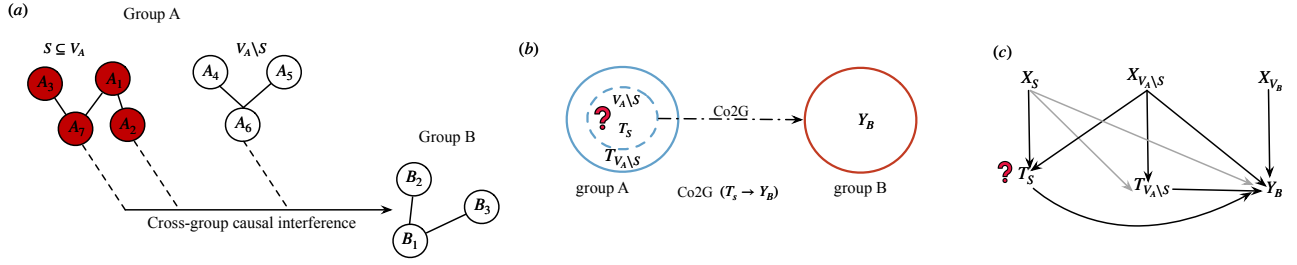


Figure 2: Cross-group causal structure and network-to-causal abstraction. (a) Network representation conditioned on a candidate subset $S \subseteq V_A$, with source units partitioned into the intervened subset S and remaining units $V_A \setminus S$. (b) The core-to-group causal effect (Co2G), contrasting the target group outcome Y_B under intervention versus non-intervention on S . (c) Corresponding causal graph with subset-level variables: $X_S, X_{V_A \setminus S}, X_{V_B}$ (pre-treatment covariates), $T_S, T_{V_A \setminus S}$ (treatment assignments), and Y_B (target outcomes).

where $t_0 = 0$ denotes the baseline intervention level for the remaining source nodes.

Core-to-Group Causal Effect. The *core-to-group causal effect* (Co2G) of subset S is defined as the contrast between two interventional target-group means:

$$\text{Co2G}(S) := \mu_B(1; S) - \mu_B(0; S). \quad (2)$$

Cross-Group Causal Influence Maximization. Given an intervention budget K , the cross-group causal influence maximization problem seeks to identify

$$S^* = \arg \max_{S \subseteq V_A, |S| \leq K} \text{Co2G}(S), \quad (3)$$

that is, to select at most K source nodes whose joint intervention yields the largest causal improvement in the outcomes of the target group B .

We state the standard assumptions commonly adopted in causal inference to support the identification results presented in the subsequent sections.

Assumption 3.1 (Markov Property [24]). Let \mathcal{G} denote the directed acyclic graph (DAG) corresponding to the causal abstraction in Fig. 2. The joint distribution over the observed variables satisfies the Markov property with respect to \mathcal{G} , i.e., each variable is independent of its non-descendants given its parents in \mathcal{G} .

Assumption 3.2 (Faithfulness [29]). The observed data distribution is faithful to the causal graph \mathcal{G} , meaning that all and only the conditional independence relationships implied by \mathcal{G} hold in the distribution.

Assumption 3.3 (Causal Sufficiency [24]). All common causes of the observed variables in the causal graph \mathcal{G} are observed. In particular, there are no unobserved confounders jointly affecting the treatment assignments in V_A and the target outcomes in V_B after conditioning on observed covariates.

Assumption 3.4 (Positivity [24]). For any subset $S \subseteq V_A$ with $|S| \leq K$, any treatment level $t \in \{0, 1\}$, and any covariate realization x with $p(X = x) > 0$, we assume $\Pr(T_S = t, T_{V_A \setminus S} = t_0 \mid X = x) > 0$, where $t_0 = 0$ denotes the baseline intervention level.

4 Method

In this section, we present the full framework for cross-group causal effect estimation and optimization. We first establish the nonparametric identifiability of the Co2G from observational data (Section 4.1), then develop a learning-based estimator and optimization procedure consisting of three components: (1) a graph neural network estimator that captures cross-group interference patterns (Section 4.2), (2) an uncertainty-aware optimization objective that guards against out-of-distribution predictions (Section 4.3), and (3) two scalable search algorithms for subset selection (Section 4.4).

4.1 Identifiability of the Cross-Group Causal Effect

We now establish the identifiability of the interventional target-group mean $\mu_B(t; S)$ and the corresponding core-to-group causal effect $\text{Co2G}(S)$ defined in Eqs. (1)–(2) under the cross-group causal structure illustrated in Fig. 2. Let $X = (X_{V_A}, X_{V_B})$ denote the collection of observed pre-treatment covariates, where X_{V_A} denotes covariates of source-group nodes, and X_{V_B} denotes covariates of target-group nodes. By construction, all variables in X are measured prior to treatment assignment and are not affected by any intervention.

Our goal is to identify, from observational data, the interventional mean $\mu_B(t; S) = \mathbb{E}[Y_B \mid \text{do}(T_S = t), \text{do}(T_{V_A \setminus S} = t_0)]$, for any subset $S \subseteq V_A$ with $|S| \leq K$ and treatment level $t \in \{0, 1\}$, where $t_0 = 0$ denotes the baseline intervention level.

Theorem 4.1 (Identifiability of the Interventional Target-Group Mean). *Under Assumptions 3.1 to 3.4 and the causal graph in Fig. 2, the interventional target-group mean $\mu_B(t; S)$ is identifiable from the observational distribution $p(X, T_{V_A}, Y_B)$ and admits the following representation:*

$$\mu_B(t; S) = \sum_x \mathbb{E}[Y_B \mid T_S = t, T_{V_A \setminus S} = t_0, X = x] p(X = x). \quad (4)$$

PROOF. Starting from the definition of the interventional distribution, $P(y_B \mid \text{do}(T_S = t), \text{do}(T_{V_A \setminus S} = t_0))$. By the law of total probability, we have $P(y_B \mid \text{do}(T_S = t), \text{do}(T_{V_A \setminus S} = t_0)) = \sum_x P(y_B \mid X = x, \text{do}(T_S = t), \text{do}(T_{V_A \setminus S} = t_0)) \times P(X = x \mid \text{do}(T_S = t), \text{do}(T_{V_A \setminus S} = t_0))$. Based on Rule 3 of do-calculus, we have $P(X = x \mid \text{do}(T_S =$

t), $\text{do}(T_{V_A \setminus S} = t_0)) = P(X = x \mid \text{do}(T_S = t))$, since $X \perp\!\!\!\perp T_{V_A \setminus S} \mid T_S$ in $\mathcal{G}_{\overline{T_S}, \overline{T_{V_A \setminus S}}}$, where \overline{T} denotes the removal of all incoming edges into T . Applying Rule 3 again yields $P(X = x \mid \text{do}(T_S = t)) = P(X = x)$, because $X \perp\!\!\!\perp T_S$ in $\mathcal{G}_{\overline{T_S}}$.

Next, by Rule 2 of do-calculus, we have $P(y_B \mid X = x, \text{do}(T_S = t), \text{do}(T_{V_A \setminus S} = t_0)) = P(y_B \mid X = x, \text{do}(T_S = t), T_{V_A \setminus S} = t_0)$ because $Y_B \perp\!\!\!\perp T_{V_A \setminus S} \mid (T_S, X)$ in $\mathcal{G}_{\overline{T_S}, \overline{T_{V_A \setminus S}}}$, where \overline{T} denotes the removal of all outgoing edges from T . Similarly, $P(y_B \mid X = x, \text{do}(T_S = t), T_{V_A \setminus S} = t_0) = P(y_B \mid X = x, T_S = t, T_{V_A \setminus S} = t_0)$, because $Y_B \perp\!\!\!\perp T_S \mid (T_{V_A \setminus S}, X)$ in $\mathcal{G}_{\overline{T_S}}$. Combining the above results, we obtain the identification formula $P(y_B \mid \text{do}(T_S = t), \text{do}(T_{V_A \setminus S} = t_0)) = \sum_x P(y_B \mid X = x, T_S = t, T_{V_A \setminus S} = t_0) P(X = x)$. \square

Corollary 4.2 (Identifiability of the Core-to-Group Causal Effect). *For any subset $S \subseteq V_A$ with $|S| \leq K$, the core-to-group causal effect $\text{Co2G}(S) = \mu_B(1; S) - \mu_B(0; S)$ is identifiable and can be expressed as*

$$\begin{aligned} \text{Co2G}(S) = \sum_x \left(\mathbb{E}[Y_B \mid T_S = 1, T_{V_A \setminus S} = t_0, X = x] \right. \\ \left. - \mathbb{E}[Y_B \mid T_S = 0, T_{V_A \setminus S} = t_0, X = x] \right) p(X = x). \end{aligned} \quad (5)$$

4.2 Causal Effect Estimator

As established in section 4.1, the interventional target-group mean $\mu_B(t; S)$ and the core-to-group causal effect $\text{Co2G}(S)$ are identifiable from observational data under Assumptions 3.1 to 3.4. We now introduce a parameterized estimator designed to approximate these identified causal quantities from networked observational data.

Estimator Overview. Let f_θ denote a learned causal effect estimator. Given a subset $S \subseteq V_A$ and a treatment level $t \in \{0, 1\}$, we represent the corresponding joint intervention $\text{do}(T_S = t, T_{V_A \setminus S} = t_0)$ by a binary treatment vector $T(S, t) \in \{0, 1\}^{|V_A|}$, where

$$T_i(S, t) = \begin{cases} t, & i \in S, \\ t_0, & i \in V_A \setminus S, \end{cases} \quad t_0 = 0. \quad (6)$$

The estimator f_θ takes as input the network structure, node covariates, and the subset-induced treatment vector $T(S, t)$, and outputs a prediction of the corresponding interventional target-group mean:

$$\widehat{\mu}_B(t; S) = f_\theta(T(S, t)). \quad (7)$$

The estimated core-to-group causal effect is then given by

$$\widehat{\text{Co2G}}(S) = \widehat{\mu}_B(1; S) - \widehat{\mu}_B(0; S). \quad (8)$$

Model Architecture. The estimator f_θ is implemented as a graph-based neural architecture that explicitly models how subset-level interventions on the source group propagate to outcomes in the target group. The architecture consists of three components. **(i) Source-group encoder.** For each source node $i \in V_A$, we construct an input representation by concatenating its observed covariates X_i with the subset-induced treatment indicator $T_i(S, t)$. A graph neural network (GNN) [31] is then applied to the induced subgraph of V_A to produce context-aware node embeddings that capture both within-group dependencies and the direct effect of the intervention. **(ii) Cross-group interference aggregation.** To model cross-group spillovers,

we propagate information from source nodes to target nodes along cross-group edges. For each target node $j \in V_B$, we aggregate the representations of its *source-group neighbors* in V_A along cross-group edges. Specifically, let $N_A(j) = \{i \in V_A : (i, j) \in E_{AB}\}$ denote the set of source nodes connected to j . A permutation-invariant aggregation operator is applied over $\{h_i : i \in N_A(j)\}$ to produce an interference representation m_j , which summarizes the spillover effect from the source group to node j . In our implementation, we use mean pooling for aggregation, i.e., $m_j = \frac{1}{|N_A(j)|} \sum_{i \in N_A(j)} h_i$. **(iii) Target outcome prediction.** The aggregated interference signal is combined with the covariates of target node j and passed through a prediction network to obtain a predicted outcome $\widehat{Y}_j(t; S)$. The estimated interventional target-group mean is then computed as

$$\widehat{\mu}_B(t; S) = \frac{1}{|V_B|} \sum_{j \in V_B} \widehat{Y}_j(t; S), \quad (9)$$

which serves as the model-based approximation of $\mu_B(t; S)$.

4.3 Uncertainty-Aware Optimization Objective

Given the estimator $\widehat{\text{Co2G}}(S)$, a natural approach would be to select the subset S that maximizes the predicted causal effect. However, since f_θ is learned from finite observational data, predictions for subsets that are far from the support of the observed data may suffer from high epistemic uncertainty.

To account for this uncertainty, we adopt a risk-averse optimization criterion based on a lower confidence bound (LCB). For a candidate subset $S \subseteq V_A$, we perform M stochastic forward passes using Monte Carlo dropout [8] and obtain samples $\{\widehat{\text{Co2G}}^{(m)}(S)\}_{m=1}^M$. We compute the empirical mean and standard deviation as follows:

$$\widehat{\mu}_{\text{Co2G}}(S) = \frac{1}{M} \sum_{m=1}^M \widehat{\text{Co2G}}^{(m)}(S), \quad (10)$$

$$\widehat{\sigma}_{\text{Co2G}}(S) = \sqrt{\frac{1}{M} \sum_{m=1}^M \left(\widehat{\text{Co2G}}^{(m)}(S) - \widehat{\mu}_{\text{Co2G}}(S) \right)^2}. \quad (11)$$

The uncertainty-aware objective is defined as

$$J(S) = \widehat{\mu}_{\text{Co2G}}(S) - \lambda \widehat{\sigma}_{\text{Co2G}}(S), \quad (12)$$

where $\lambda \geq 0$ controls the strength of uncertainty penalization. Maximizing $J(S)$ favors subsets with large predicted causal effects while discouraging selections associated with high uncertainty.

4.4 Subset Selection Algorithms

Greedy Search. For small to medium-sized networks, we adopt an iterative greedy procedure to approximately solve $\max_{S \subseteq V_A} J(S)$ subject to $|S| \leq K$. Starting from the empty set $S_0 = \emptyset$, at iteration k we select the node that yields the largest marginal improvement in the uncertainty-aware objective:

$$v^* = \arg \max_{v \in V_A \setminus S_{k-1}} [J(S_{k-1} \cup \{v\}) - J(S_{k-1})]. \quad (13)$$

If the maximum marginal gain is positive, we update $S_k = S_{k-1} \cup \{v^*\}$; otherwise, the procedure terminates early. The algorithm stops once $|S_k| = K$ or no further improvement is possible. The full procedure is summarized in Algorithm 1.

Algorithm 1 Uncertainty-Aware Greedy Search (*CauMax-G*)

Input: Trained estimator f_θ ; source nodes V_A ; budget K ; MC passes M ; uncertainty penalty λ

Output: Selected subset S

- 1: $S \leftarrow \emptyset$
- 2: Estimate $J(S) = \widehat{\mu}_{\text{Co2G}}(S) - \lambda \widehat{\sigma}_{\text{Co2G}}(S)$ using M MC-dropout passes
- 3: **for** $k = 1$ to K **do**
- 4: $\Delta^* \leftarrow -\infty, v^* \leftarrow \text{None}$
- 5: **for all** $v \in V_A \setminus S$ **do**
- 6: Estimate $J(S \cup \{v\})$ using M MC-dropout passes
- 7: $\Delta \leftarrow J(S \cup \{v\}) - J(S)$
- 8: **if** $\Delta > \Delta^*$ **then**
- 9: $\Delta^* \leftarrow \Delta$
- 10: $v^* \leftarrow v$
- 11: **end if**
- 12: **end for**
- 13: **if** $\Delta^* > 0$ **then**
- 14: $S \leftarrow S \cup \{v^*\}$
- 15: Update cached $J(S)$
- 16: **else**
- 17: **break**
- 18: **end if**
- 19: **end for**
- 20: **return** S

Differentiable Subset Optimization. For large-scale source groups, the greedy procedure in Algorithm 1 becomes computationally expensive due to repeated evaluations of $J(S)$. To address this limitation, we introduce a differentiable relaxation that enables gradient-based optimization of the same uncertainty-aware objective.

Instead of directly optimizing over discrete subsets, we relax the subset indicator to a continuous vector and optimize a smooth surrogate of $J(S)$ while enforcing the budget constraint. After optimization, a discrete subset is recovered via a top- K projection. The resulting procedure is summarized in Algorithm 2.

Each source node $i \in V_A$ is associated with a learnable logit ψ_i . A relaxed treatment vector $\tilde{T} \in [0, 1]^{|V_A|}$ is generated via a Gumbel-Softmax reparameterization [14], which can be interpreted as a soft approximation of a subset-induced intervention. The estimator f_θ is kept fixed, and the logits ψ are optimized to maximize the uncertainty-aware objective under a budget constraint:

$$\min_{\psi} -\mathbb{E}_{g \sim \text{Gumbel}} [J(\tilde{T}(\psi, g))] + \gamma \left(\|\tilde{T}(\psi, g)\|_1 - K \right)^2, \quad (14)$$

where $\tilde{T}(\psi, g) = \sigma((\psi + g)/\tau)$ is the Gumbel-Softmax relaxation and the expectation is taken over the Gumbel noise g . After optimization, a discrete subset S is obtained by selecting the top- K nodes according to ψ . This approach scales linearly with $|V_A|$ and is suitable for large-scale networks.

5 Experiments

We evaluate the proposed framework on two real-world social networks, BlogCatalog (BC) and Flickr. Our experiments address three

Algorithm 2 Differentiable Gradient Search (*CauMax-D*)

Input: Effect estimator f_θ ; source nodes V_A ; budget K ; iterations M_{iter} ; learning rate η ; MC passes M ; uncertainty penalty λ ; regularization γ

Output: Selected subset S_K

- 1: Initialize $\psi \sim \mathcal{N}(0, 0.01I)$
- 2: **for** $m = 1$ to M_{iter} **do**
- 3: Sample $g \sim \text{Gumbel}(0, 1)^{|V_A|}$
- 4: Generate soft mask $\tilde{T} \leftarrow \sigma((\psi + g)/\tau) \triangleright \tilde{T} \in [0, 1]^{|V_A|}$ is a continuous relaxation of the subset indicator
- 5: Estimate $\widehat{\mu}_{\text{Co2G}}(\tilde{T})$ and $\widehat{\sigma}_{\text{Co2G}}(\tilde{T})$ using M MC-dropout passes
- 6: $J(\tilde{T}) \leftarrow \widehat{\mu}_{\text{Co2G}}(\tilde{T}) - \lambda \widehat{\sigma}_{\text{Co2G}}(\tilde{T})$
- 7: $\mathcal{L} \leftarrow -J(\tilde{T}) + \gamma \left(\|\tilde{T}\|_1 - K \right)^2$
- 8: $\psi \leftarrow \psi - \eta \nabla_{\psi} \mathcal{L}$
- 9: **end for**
- 10: $S_K \leftarrow \text{TOPK_INDICES}(\psi, K)$
- 11: **return** S_K

questions: (i) whether the proposed estimator accurately recovers cross-group causal effects, (ii) whether uncertainty-aware selection reduces regret over heuristic baselines, and (iii) how the two optimization strategies compare across network sizes.

5.1 Baselines

We compare against: *Random*, which selects K source nodes uniformly at random [17]; *Degree*, which selects the K highest-degree source nodes [18]; and *Influence Maximization (IM)*, which selects nodes to maximize diffusion-based cascade spread without considering causal effects [20]. We evaluate two variants of *CauMax*: *CauMax-G* (Algorithm 1), an iterative greedy search, and *CauMax-D* (Algorithm 2), a differentiable gradient-based method with Top- K projection.

5.2 Evaluation Metrics

Approximate Oracle Subset (S_k^).* To assess the quality of a selected subset, we construct an approximate oracle solution using access to the ground-truth causal effect. For a fixed budget k , the oracle subset is defined as $S_k^* = \arg \max_{S \subseteq V_A, |S|=k} \text{Co2G}(S)$, where $\text{Co2G}(S)$ denotes the true core-to-group causal effect computed from the data-generating process. Since exhaustive enumeration over all $\binom{|V_A|}{k}$ subsets is computationally infeasible, we approximate S_k^* using a greedy procedure that incrementally adds the source node with the largest marginal increase in the true $\text{Co2G}(\cdot)$. This procedure, referred to as *Oracle-Greedy*, serves as a computationally tractable proxy for the true oracle and is used only for evaluation purposes.

Regret@k. Given a method that returns a subset S_k of size k , we define the regret as $\text{Regret}@k = \text{Co2G}(S_k^*) - \text{Co2G}(S_k)$, which measures the performance gap between the selected subset and the approximate oracle. Lower regret indicates that the selected subset achieves a causal effect closer to the oracle solution.

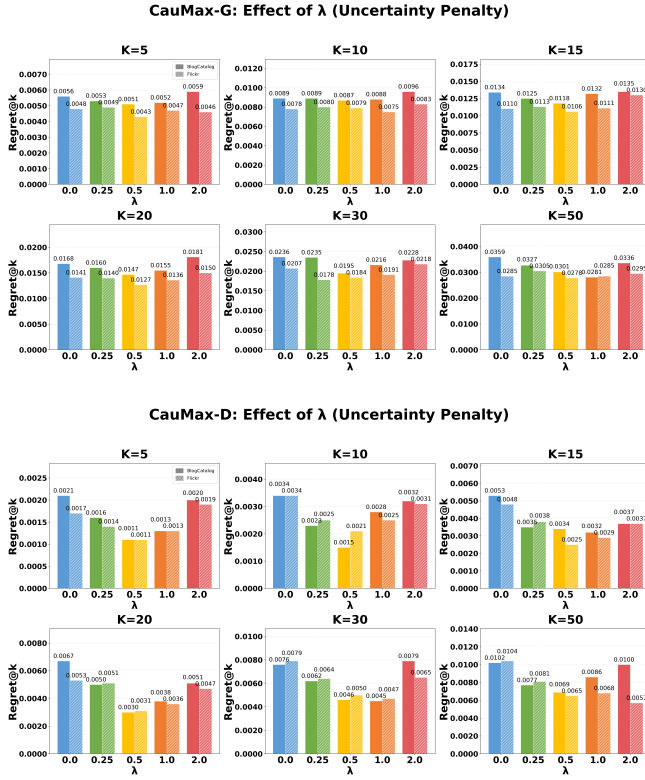


Figure 3: Sensitivity analysis of the uncertainty penalty λ on $\text{Regret}@K$ across both datasets and all budget levels $K \in \{5, 10, 15, 20, 30, 50\}$. Solid bars represent BC and hatched bars represent Flickr.

Estimation Error. In addition to subset-level performance, we evaluate the accuracy of the causal effect estimator by computing the root mean squared error (RMSE) between the estimated and true core-to-group causal effects over a collection of evaluated subsets \mathcal{S} : $\text{RMSE} = \sqrt{\frac{1}{|\mathcal{S}|} \sum_{S \in \mathcal{S}} (\widehat{\text{Co2G}}(S) - \text{Co2G}(S))^2}$.

5.3 Main Results

Table 2 compares all methods on BC and Flickr at $\lambda = 0.5$ with the proposed methods. We make the following key observations.

The proposed methods substantially outperform all baselines. Across all budget levels $K \in \{5, 10, 15, 20, 30, 50\}$, both proposed methods achieve markedly lower regret than Degree, IM, and Random. For instance, at $K = 20$ on BC, CauMax-D achieves $\text{Regret}@K = 0.0030$, compared with 0.0338 for Degree, 0.0576 for IM, and 0.0783 for Random, an order-of-magnitude improvement. This confirms that explicitly optimizing a causal estimand leads to more effective cross-group interventions than relying on structural heuristics or diffusion-based objectives.

CauMax-D closely tracks the oracle. CauMax-D consistently achieves the lowest regret across both datasets and all budget levels, closely approximating the oracle-greedy solution. On Flickr, CauMax-D

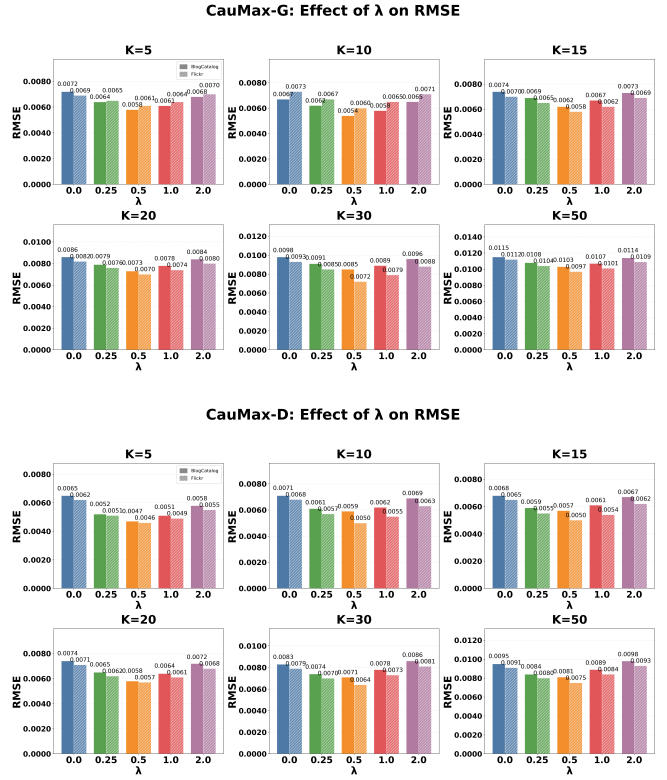


Figure 4: Sensitivity analysis of the uncertainty penalty λ on RMSE.

maintains regret at most 0.0065 even at $K = 50$, whereas CauMax-G reaches 0.0278 and baselines exceed 0.05. The advantage of CauMax-D is particularly pronounced at larger budgets, where the combinatorial search space makes greedy selection more susceptible to local optima.

Estimation accuracy correlates with subset selection quality. The RMSE results in Table 2 show a ranking broadly aligned with $\text{Regret}@K$: across most budget levels, CauMax-D achieves the lowest RMSE, followed by CauMax-G, Degree, IM, and Random. This indicates that better causal effect estimation directly translates to better subset selection.

5.4 Sensitivity to the Uncertainty Penalty λ

We vary $\lambda \in \{0, 0.25, 0.5, 1.0, 2.0\}$, where $\lambda = 0$ reduces to the mean-only baseline, as shown in Figs. 3 and 4. Moderate penalization ($\lambda \in [0.25, 0.5]$) consistently reduces regret across both datasets and search strategies; for CauMax-D, $\lambda = 0.5$ reduces regret by up to 42% relative to $\lambda = 0$. However, excessive penalization ($\lambda = 2.0$) degrades performance by favoring low-variance subsets with smaller predicted effects. CauMax-D exhibits a stable U-shaped response with a clear optimum around $\lambda = 0.5$, while CauMax-G shows a flatter profile, suggesting its iterative selection partially compensates for estimation noise even without explicit uncertainty penalization.

Table 2: Comparison of Regret@K and RMSE across methods on BC and Flickr ($\lambda = 0.5$ for CauMax-D and CauMax-G). Bold indicates the best result; underline indicates the second best.

Method	Dataset	Regret@K (\downarrow)						RMSE (\downarrow)					
		k=5	k=10	k=15	k=20	k=30	k=50	k=5	k=10	k=15	k=20	k=30	k=50
CauMax-D	BC	0.0011	0.0015	0.0034	0.0030	0.0046	0.0069	0.0047	<u>0.0059</u>	0.0057	0.0058	0.0071	0.0081
	Flickr	0.0011	0.0021	0.0025	0.0031	0.0050	0.0065	0.0046	0.0050	0.0050	0.0057	0.0064	0.0075
CauMax-G	BC	<u>0.0051</u>	<u>0.0087</u>	<u>0.0118</u>	<u>0.0147</u>	<u>0.0195</u>	<u>0.0301</u>	<u>0.0058</u>	0.0054	<u>0.0062</u>	<u>0.0073</u>	<u>0.0085</u>	<u>0.0103</u>
	Flickr	<u>0.0043</u>	<u>0.0079</u>	<u>0.0106</u>	<u>0.0127</u>	<u>0.0184</u>	<u>0.0278</u>	<u>0.0061</u>	<u>0.0060</u>	<u>0.0058</u>	<u>0.0070</u>	<u>0.0072</u>	<u>0.0097</u>
Degree	BC	0.0111	0.0204	0.0280	0.0338	0.0483	0.0657	0.0096	0.0102	0.0104	0.0115	0.0132	0.0169
	Flickr	0.0101	0.0158	0.0235	0.0265	0.0415	0.0588	0.0097	0.0094	0.0110	0.0114	0.0130	0.0163
IM	BC	0.0201	0.0341	0.0427	0.0576	0.0799	0.1218	0.0137	0.0134	0.0157	0.0163	0.0181	0.0229
	Flickr	0.0162	0.0293	0.0388	0.0474	0.0732	0.0999	0.0126	0.0132	0.0141	0.0151	0.0175	0.0215
Random	BC	0.0274	0.0449	0.0646	0.0783	0.1130	0.1622	0.0189	0.0200	0.0199	0.0216	0.0246	0.0301
	Flickr	0.0228	0.0378	0.0558	0.0711	0.0941	0.1373	0.0172	0.0189	0.0194	0.0218	0.0228	0.0300

Table 3: Comparison of time complexity for subset selection methods.

Method	Time Complexity
CauMax-G (Alg. 1)	$O(K \cdot V_A \cdot M \cdot T_{\text{model}})$
CauMax-D (Alg. 2)	$O(E_{\text{opt}} \cdot M \cdot T_{\text{model}})$
Degree	$O(V_A \log V_A + E)$
IM	$O(K \cdot V_A \cdot R \cdot E)$
Random	$O(K)$

5.5 Computational Complexity

We analyze the time complexity of the proposed algorithms compared to the baselines, as summarized in Table 3. Let $|V_A|$ denote the number of source nodes, $|E|$ the number of edges, K the budget, and T_{model} the cost of a single forward pass through the estimator f_{θ} . For the stochastic methods, M represents the number of Monte Carlo dropout passes, and R denotes the diffusion simulations in IM.

The **CauMax-G** (Algorithm 1) is computationally intensive; it requires K iterations, where each iteration evaluates $|V_A| - |S|$ candidates via M stochastic forward passes. This results in a complexity of $O(K \cdot |V_A| \cdot M \cdot T_{\text{model}})$. In contrast, the **CauMax-D** (Algorithm 2) runs for a fixed number of gradient steps E_{opt} , independent of the candidate set size during optimization, yielding $O(E_{\text{opt}} \cdot M \cdot T_{\text{model}})$. Since $E_{\text{opt}} \ll K \cdot |V_A|$ in practice, the differentiable method achieves a substantial speedup. Regarding baselines, **Degree** is highly efficient with $O(|V_A| \log |V_A| + |E|)$ due to sorting, while **IM** is expensive, scaling with the number of simulations R and graph size.

6 Conclusion

We introduced the problem of cross-group causal influence maximization, which seeks to identify the subset of source-group units whose intervention yields the greatest causal improvement in outcomes of a distinct target group connected through network interference pathways. We defined the core-to-group causal effect

(Co2G) as a causal estimand grounded in the potential outcomes framework, and established its nonparametric identifiability from observational data via do-calculus. Building on this identification result, we proposed CauMax, a framework combining a graph neural network-based estimator that models within-group dependencies and cross-group spillover propagation with an uncertainty-aware optimization objective, instantiated through two scalable algorithms: CauMax-G (greedy search) and CauMax-D (differentiable optimization). Experiments on social network datasets confirmed that CauMax yields substantially lower regret than structural heuristics and diffusion-based baselines.

Limitations and Future Work. Our identification and estimation framework relies on the causal sufficiency assumption (Assumption 3.3), which requires that all common causes of source-group treatments and target-group outcomes are observed. In practice, unmeasured confounders such as latent homophily or unobserved socioeconomic factors may bias the estimated Co2G. Addressing hidden confounding is not the focus of this work, but it constitutes an important direction for future research. Potential approaches include incorporating proxy variables, instrumental variable methods, or sensitivity analysis to bound the impact of unobserved confounders on the estimated cross-group causal effects.

References

- [1] Roy M. Anderson and Robert M. May. 1991. *Infectious Diseases of Humans: Dynamics and Control*. Oxford University Press, Oxford.
- [2] Peter M. Aronow and Cyrus Samii. 2017. Estimating average causal effects under general interference. *Annals of Applied Statistics* 11, 4 (2017), 1912–1947.
- [3] Marie Claude Boily, C Lowndes, and M Alary. 2002. The impact of HIV epidemic phases on the effectiveness of core group interventions: insights from mathematical models. *Sexually Transmitted Infections* 78, suppl 1 (2002), i78–i90.
- [4] Ruichu Cai, Zhimeng Yang, Wei Chen, Yuhan Yan, and Zhifeng Hao. 2023. Generalization bound for estimating causal effects from observational network data. In *Proceedings of the 32nd ACM International Conference on Information and Knowledge Management*. Association for Computing Machinery, New York, NY, USA, 163–172.
- [5] Wei Chen, Yajun Wang, and Siyu Yang. 2009. Efficient influence maximization in social networks. In *Proceedings of the 15th ACM SIGKDD international conference on Knowledge discovery and data mining*. Association for Computing Machinery, New York, NY, USA, 199–208.

- [6] Shiru Cui and Xuzhen Zhu. 2024. The information propagation mechanism of individual heterogeneous adoption behavior under the heterogeneous network. *Frontiers in Physics* 12 (2024), 1404464.
- [7] Laura Forastiere, Edoardo M Airoidi, and Fabrizia Mealli. 2021. Identification and estimation of treatment and interference effects in observational studies on networks. *J. Amer. Statist. Assoc.* 116, 534 (2021), 901–918.
- [8] Yarin Gal and Zoubin Ghahramani. 2016. Dropout as a bayesian approximation: Representing model uncertainty in deep learning. In *International Conference on Machine Learning*. PMLR, New York, New York, USA, 1050–1059.
- [9] Kevin Han, Shuangning Li, Jialiang Mao, and Han Wu. 2023. Detecting interference in online controlled experiments with increasing allocation. In *Proceedings of the 29th ACM SIGKDD Conference on Knowledge Discovery and Data Mining*. Association for Computing Machinery, New York, NY, USA, 661–672.
- [10] Chris Heitzig and Rossa O’Keeffe-O’Donovan. 2024. Spillover effects and diffusion of savings groups. *World Development* 173 (2024), 106377.
- [11] Michael G. Hudgens and M. Elizabeth Halloran. 2008. Toward causal inference with interference. *J. Amer. Statist. Assoc.* 103, 482 (2008), 832–842.
- [12] Kosuke Imai, Zhichao Jiang, and Anup Malani. 2021. Causal inference with interference and noncompliance in two-stage randomized experiments. *J. Amer. Statist. Assoc.* 116, 534 (2021), 632–644.
- [13] Guido W Imbens and Donald B Rubin. 2015. *Causal inference in statistics, social, and biomedical sciences*. Cambridge University Press, Cambridge.
- [14] Eric Jang, Shixiang Gu, and Ben Poole. 2017. Categorical Reparameterization with Gumbel-Softmax. In *5th International Conference on Learning Representations, ICLR*. OpenReview.net, Toulon, France, 1–12.
- [15] Li Ji, Xingyu Chen, Ling Jiang, and Justin T Huang. 2025. Within-and cross-group spillover effects in influencer marketing: The heterogeneity between micro-and macro-influencers. *Information & Management* 62, 7 (2025), 104202.
- [16] Sheng Jiang and Yizhou Sun. 2022. Estimating causal effects on networked observational data via representation learning. In *Proceedings of the 31st ACM International Conference on Information & Knowledge Management*. Association for Computing Machinery, New York, NY, USA, 852–861.
- [17] David Kempe, Jon Kleinberg, and Éva Tardos. 2003. Maximizing the spread of influence through a social network. In *Proceedings of the Ninth ACM SIGKDD International Conference on Knowledge Discovery and Data Mining*. Association for Computing Machinery, New York, NY, USA, 137–146.
- [18] Dror Y Kenett, Matjaž Perc, and Stefano Boccaletti. 2015. Networks of networks—an introduction. *Chaos, Solitons & Fractals* 80 (2015), 1–6.
- [19] Youjin Lee, Ashley L Buchanan, Elizabeth L Ogburn, Samuel R Friedman, M Elizabeth Halloran, Natallia V Katenka, Jing Wu, and Georgios K Nikolopoulos. 2023. Finding influential subjects in a network using a causal framework. *Biometrics* 79, 4 (2023), 3715–3727.
- [20] Jure Leskovec, Andreas Krause, Carlos Guestrin, Christos Faloutsos, Jeanne VanBriesen, and Natalie Glance. 2007. Cost-effective outbreak detection in networks. In *Proceedings of the 13th ACM SIGKDD International Conference on Knowledge Discovery and Data Mining*. Association for Computing Machinery, New York, NY, USA, 420–429.
- [21] Jing Ma, Chen Chen, Anil Vullikanti, Ritwick Mishra, Gregory Madden, Daniel Borrajo, and Jundong Li. 2023. A look into causal effects under entangled treatment in graphs: Investigating the impact of contact on mrsa infection. In *Proceedings of the 29th ACM SIGKDD Conference on Knowledge Discovery and Data Mining*. Association for Computing Machinery, New York, NY, USA, 4584–4594.
- [22] Edward Miguel and Michael Kremer. 2004. Worms: identifying impacts on education and health in the presence of treatment externalities. *Econometrica* 72, 1 (2004), 159–217.
- [23] Elizabeth L. Ogburn, Oleg Sofrygin, Ivan Diaz, and Mark J. Van der Laan. 2024. Causal inference for social network data. *J. Amer. Statist. Assoc.* 119, 545 (2024), 597–611.
- [24] Jude Pearl. 2009. *Causality*. Cambridge University Press, Cambridge.
- [25] Clemens Possnig, Andreea Rotărescu, and Kyungchul Song. 2022. Estimating dynamic spillover effects along multiple networks in a Linear panel model. arXiv:2211.08995
- [26] Donald B Rubin. 2005. Causal inference using potential outcomes: Design, modeling, decisions. *Journal of the American statistical Association* 100, 469 (2005), 322–331.
- [27] Tiago A Schieber, Laura C Carpi, Panos M Pardalos, Cristina Masoller, Albert Diaz-Guilera, and Martín G Ravetti. 2023. Diffusion capacity of single and interconnected networks. *Nature Communications* 14, 1 (2023), 2217.
- [28] Michael E Sobel. 2006. What do randomized studies of housing mobility demonstrate? Causal inference in the face of interference. *J. Amer. Statist. Assoc.* 101, 476 (2006), 1398–1407.
- [29] Peter Spirtes, Clark N Glymour, and Richard Scheines. 2000. *Causation, prediction, and search*. MIT Press, Cambridge, MA.
- [30] Xinyan Su, Zhiheng Zhang, Jiyuan Qiu, Zhaojuan Yue, and Jun Li. 2025. Unveiling environmental sensitivity of individual gains in influence maximization. In *The Thirty-ninth Annual Conference on Neural Information Processing Systems*. Curran Associates, Inc., Red Hook, NY, 1–14.
- [31] Zonghan Wu, Shirui Pan, Fengwen Chen, Guodong Long, Chengqi Zhang, and Philip S Yu. 2020. A comprehensive survey on graph neural networks. *IEEE Transactions on Neural Networks and Learning Systems* 32, 1 (2020), 4–24.
- [32] Wenjing Yang, Haotian Wang, Haoxuan Li, Hao Zou, Ruochun Jin, Kun Kuang, and Peng Cui. 2024. Your neighbor matters: Towards fair decisions under networked interference. In *Proceedings of the 30th ACM SIGKDD Conference on Knowledge Discovery and Data Mining*. Association for Computing Machinery, New York, NY, USA, 3829–3840.
- [33] Yuan Yuan, Kristen Altenburger, and Farshad Kooti. 2021. Causal network motifs: Identifying heterogeneous spillover effects in a/b tests. In *Proceedings of the Web Conference 2021*. Association for Computing Machinery, New York, NY, USA, 3359–3370.